L-type calcium channel contribution to striatal dopamine release is governed by calbindin-D28K, the dopamine transporter, D2-receptors, $\alpha_2\delta$-subunits and sex differences

Katherine R. Brimblecombe*[1,2], Natalie Connor-Robson[1,2], Bradley M. Roberts[1,2], Caitlin Gracie[1], Rebecca te Water Naude[1], Gayathri Karthik[1], Richard Wade-Martins[1,2], Stephanie J. Cragg[1,2]

ORCID IDs: KRB 0000-0003-0809-7292; NCR 0000-0001-8350-6928; BMR 0000-0002-5192-2545; RtWN 0000-0002-1350-3163; GC 0000-0003-1876-0975; RWM 0000-0001-6691-580X; SJC 0000-0001-9677-2256

Affiliations:

[1]Department of Physiology, Anatomy and Genetics, University of Oxford, OX1 3PT, UK

[2]Oxford Parkinson's Disease Centre, University of Oxford, Oxford, United Kingdom

***Correspondence should be addressed to:**

Dr Katherine Brimblecombe

Department of Physiology, Anatomy & Genetics

University of Oxford, OX1 3PT Oxford, UK

Email: katherine.brimblecombe@dpag.ox.ac.uk

Abstract

Ca^{2+} entry to nigrostriatal dopamine (DA) neurons and axons via L-type voltage-gated Ca^{2+} channels (LTCCs) contributes to pacemaker activity and DA release, but burdens cells with a metabolic stress promoting their vulnerability to parkinsonian degeneration. The level of LTCC function varies between subtypes of DA neurons, but is not proportional to LTCC expression level, indicating that LTCC function is governed by other factors. We used fast-scan cyclic voltammetry in mouse brain slices to identify mechanisms that govern whether LTCCs contribute to DA release in dorsal and ventral striatum. We find that calbindin-D28K limits LTCC function in a regionally and sexually divergent manner; D2-receptors and DA transporters are negative and positive regulators respectively; and lastly, that targeting $\alpha_2\delta$ subunits with gabapentinoid drugs restricts LTCC function without compromising DA release. These data reveal that LTCC function in DA axons is dynamically and locally regulated, which may prove useful for future neuroprotective strategies.

Keywords

Dopamine release; L-type calcium channel; voltage-gated calcium channels; alpha2delta; gabapentin; pregabalin; gabapentinoids; dopamine transporter; calb1; dopamine D2 receptor; striatum; Parkinson's disease

Introduction

Ca^{2+} entry via voltage-gated Ca^{2+} channels (VGCCs) is important for pacemaker activity in DA neurons within the substantia nigra pars compacta (SNc), and for striatal DA release (Brimblecombe et al., 2015; Guzman et al., 2009). However, Ca^{2+} is also a source of metabolic stress that promotes vulnerability of nigrostriatal DA neurons to degeneration in Parkinson's disease (PD) (Surmeier et al., 2010). Axons of DA neurons that innervate dorsal striatum (caudatoputamen, CPu) primarily originate from neurons in SNc and use a wider range of VGCCs to support DA release than axons in ventral striatum (nucleus accumbens core, NAc core) (Brimblecombe et al., 2015), which primarily originate in ventral tegmental area (VTA) and are less susceptible to degeneration. The greater role of L-type VGCCs (LTCCs) in SNc than VTA DA neurons promotes their Ca^{2+}-related stress (Guzman et al., 2010). A recent clinical trial explored whether the LTCC blocker isradipine prevented PD progression but was unsuccessful (Parkinson Study Group STEADY-PD III Investigators, 2020). There are several potential explanations, including that isradipine directly decreases DA release in CPu (Brimblecombe et al., 2015). Future neuroprotective strategies to limit Ca^{2+} entry would ideally limit Ca^{2+} burden but not DA release.

The mechanisms that govern VGCC function in DA axons are not well understood. The greater role of LTCCs in axons from SNc than VTA neurons is paradoxical: LTCC expression is greater in VTA than SNc (Greene et al., 2005; Poulin et al., 2014), suggesting that other mechanisms operate differently between SNc and VTA neurons to recruit or inhibit LTCC function. Here, we probed mechanisms that govern whether LTCCs contribute to DA release. We first tested if LTCC control of DA release varies between male and female mice. Not only is there a greater incidence of PD in males than females (Wooten et al., 2004), but LTCC function is greater in males than females in cardiac myocytes (Curl et al., 2008). Secondly, we assessed whether fast Ca^{2+} buffering by calbindin-D28k (calb1) limits LTCC function. Calb1 is enriched in VTA neurons (Gerfen et al., 1987; Poulin et al., 2014), limits DA release in NAc (Brimblecombe et al., 2019) and in expression systems can bind to and limit function of LTCCs (Lee et al., 2006). Thirdly, we tested whether axonal DA D2-receptors (D2Rs) limit LTCC contribution, since D2Rs in striatal GABAergic projection neurons inhibit LTCC function (via βγ-inhibition) (Hernández-López et al., 2000; Olson et al., 2005). Fourthly, we tested whether DA uptake transporters (DATs) promote LTCC function. LTCC currents in expression systems are promoted by electrogenic monoamine transporters (Cameron et al., 2015) and DAT levels are higher in SNc than VTA neurons (Poulin et al., 2014). Finally, we explored the role of the VGCC auxiliary subunit $\alpha_2\delta$. The $\alpha_2\delta$ subunit participates in trafficking and distribution of VGCCs including LTCCs in other cell types (Andrade et al., 2009; Dolphin, 2012) and have been found to be transcriptionally enriched in SNc (Chung et al., 2005). We reveal a network of factors that inhibit or facilitate LTCC function in DA axons that contribute to greater LTCC function in CPu than NAc, and in males than females.

Results and Discussion

Sex and calbindin interact to govern LTCC function

We and others have to date principally identified LTCC function in DA neurons in males rather than females (Brimblecombe et al., 2015; Guzman et al., 2009, 2018; Ilijic et al., 2011). It is important to understand the biology of LTCCs in both sexes, in order to understand both drug action and aetiology, as there is a ~2:1 prevalence of PD in males and females. Notably, LTCC function has been shown to be sexually dimorphic in cardiac tissue, with greater function in males than females, through which it is thought to contribute to increased risk of coronary disease in men (Curl et al., 2008; Prabhavathi et al., 2014). And yet the relative roles of LTCCs in nigrostriatal DA neurons/axons in males versus females is poorly understood. Here, we first tested whether LTCCs support DA

release in CPu of female mice, as they do in male mice (Brimblecombe et al., 2015). We found that LTCC inhibitor isradipine (5 µM) decreased $[DA]_o$ evoked by single electrical stimulus pulses (1p) in CPu of male mice (**Figure 1A,** comparison of peak $[DA]_o$, t_4=5.6, *P*=0.005, N=3) as published previously (Brimblecombe et al., 2015)but not female mice (**Figure 1A,B,** comparison of peak $[DA]_o$, t_4=0.95, *P*=0.39, N=3), revealing a statistically significant difference between the two sexes (**Figure 1B,** Two-way ANOVA: sex x drug interaction, $F_{16,67}$=3.0, *P*<0.001; main effect of sex, $F_{1,67}$=44.9, *P*<0.001). We speculate that greater axonal LTCC function in males than females might contribute to the higher incidence of PD in men than women (Wooten et al., 2004). In addition, these findings reveal the importance of considering sex-dependent pharmacology in treatment strategies.

Calbindin-D28K (calbindin1, calb1) is a fast intracellular Ca^{2+} buffer expressed at higher levels in DA neurons of VTA than SNc (Chung et al., 2005; Gerfen et al., 1987; Greene et al., 2005; Poulin et al., 2014) that governs DA release from DA axons in NAc but not CPu (Brimblecombe et al., 2019). We have previously found that LTCC function in NAc can be unsilenced by increasing $[Ca^{2+}]_o$ (Brimblecombe et al., 2015), and therefore, calb1, by binding Ca^{2+}, is a candidate for limiting the contribution of LTCCs to DA release in NAc. Calb1 also limits LTCC function in other cell types (Lee et al., 2006) and intriguingly, has been shown to be enriched in females in some brain regions (cerebellum and frontal cortex)(Abel et al., 2011) providing a potentially greater means to limit LTCC function in females. We tested the hypothesis that calb1 and sex might interact to govern LTCC function. Levels of Calb1 mRNA in DA neurons are thought to be similar between males and females (Chung et al., 2017) but protein levels have not been assessed. We used western blot analysis of midbrain and striatal tissue to first assess any overall sex differences in levels of calb1 protein, but found no significant difference in calb1 levels between males and females in either midbrain or striatum (**Figure 1C,D)**, Two-way ANOVA: effect of sex, $F_{1,32}$=0.076, *P*=0.78, N=3, with technical repeats (n=9). We nonetheless explored a potential functional interaction between sex, calb1 and LTCC function in the control of striatal DA release using a mouse conditional calb1 knockdown targeted to DA neurons (CalbKD) (Brimblecombe et al., 2019). In females with wild-type calb1 on a control DAT-$Cre^{+/-}$ background (CalbWT), isradipine did not limit 1p-evoked $[DA]_o$ in CPu, as seen in wild-type mice (see Figure 1A), but in CalbKD mice, isradipine significantly reduced 1p-evoked $[DA]_o$ in CPu (**Figure 1E,** comparison of peaks, CalbWT, t_6=4.0, *P*=0.007, CalbKD, t_4=3.0, *P*=0.042), showing a significant effect of calb1 knockdown on revealing LTCC function (normalised effect of isradipine 1.09 vs 0.79, t_5=7.1, *P*=0.001, N=4 CalbWT, N=3 CalbKD). These data indicate that calb1 in CPu in females prevents LTCCs from supporting DA release in CPu in females, despite calb1 not buffering sufficient Ca^{2+} to directly limit the levels of DA released in CPu (Brimblecombe et al., 2019).

To explore whether these effects of calb1 on LTCC function in CPu in females were sex-specific, or applicable to both sexes, we explored whether calb1 also limits the LTCC control of DA release in male mice. In CPu in male mice, in calbWT and calbKD mice, isradipine decreased DA release (**Figure 1F** comparison of peaks calbWT t_4=4.8 P=0.009 calbKD t_4=5.5 P=0.005) with no significant difference in effect size between genotypes for this sample size (normalised effect of isradipine 0.76 vs 0.69 calbWT vs calbKD t_4=1.1 P=0.34 N=3), however, in NAc, where LTCC function is not normally apparent (Brimblecombe et al., 2015), there was no effect of isradipine in CalbWT mice but isradipine significantly decreased 1p-evoked $[DA]_o$ in CalbKD (**Figure 1G** comparison of peaks calbWT t_4=0.07 P=0.95 calbKD t_6=3.3 P=0.018). The effect of isradipine in NAc was significantly greater in calbKD than calbWT (normalised effect of isradipine 1.0 vs 0.78 t_5=3.3 P=0.02 N=3 calbWT N=4 calbKD) showing that calb1 limits LTCC function in NAc. This finding is consistent with previous data showing LTCC regulation of DA release can be "unsilenced" in NAc by increasing $[Ca^{2+}]_o$ presumably due to overwhelming endogenous calb1. Calb1 is therefore important for both regional and sexual differences in LTCC regulation of DA release.

The mechanisms through which sex, calb1 and LTCC interact are is likely to be complex. Sexual dimorphism in LTCC function is well documented in cardiac tissue, in which oestrogen regulates LTCC expression, localisation and function through mechanisms spanning from transcriptional to post-translational. In the brain, calb1 function can be regulated by sex-linked genes and hormones at transcriptional and protein level (Abel and Rissman, 2012), and its relevance is becoming increasingly appreciated (Vega-Vela et al., 2017). The mechanisms operating in DA neurons are not yet known but could have important implications clinically for drug action as well as vulnerability to degeneration.

DAT promotes and D2R limits LTCC control of DA release

We investigated whether D2Rs or DATs regulate the contribution of LTCCs to DA release, firstly in CPu in male wild-type mice. We inhibited D2Rs using antagonist L-741626 (1 µM), but this did not modify the effect on evoked $[DA]_o$ of LTCC inhibitor isradipine (**Figure 2A-C,** comparison of peaks t-test t_8=3.5 p=0.008 N=4), indicating that either there is either negligible tonic activation of D2Rs or no inhibition of LTCCs by D2Rs in CPu. Translocation of DA across the membrane by DAT involves the co-transport of 2 Na^+ and 1 Cl^-, an electrogenic process that can depolarise DA neuron membranes (Ingram et al., 2002) and in cellular expression systems can activate LTCCs (Cameron et al., 2015). We inhibited DATs using cocaine (5 µM), which is known to prevent the electrogenic effects of DAT (Sonders et al., 1997), and found that the effect of LTCC inhibitor isradipine on DA release in CPu were precluded: isradipine did not modify 1p-evoked $[DA]_o$ (**Figure 2A-C,** Two-way ANOVA: isradipine

x pre-condition interaction $F_{32,153}$=2.69, P<0.001; effect of isradipine $F_{16,153}$=5.53, P<0.001, Sidak post-test: cocaine vs standard pre-condition, P<0.001, comparison of peaks t-test: t_8=0.18, P=0.86, N=5). This effect of DAT inhibition was not due to an elevation of D2R activation resulting from enhanced $[DA]_o$ since the presence of D2R antagonist L-741626 did not reinstate the effects of isradipine in the presence of cocaine (**Figure 2C**). Furthermore, the loss of isradipine effect in the presence of DAT inhibition was not due to non-specific local anaesthetic effects of cocaine blocking Na_v because application of the local anaesthetic and Na_v blocker lidocaine did not reproduce this action. Rather, in the presence of lidocaine, isradipine decreased $[DA]_o$ similarly to standard control conditions (**Figure 2C,** One-way ANOVA, effect of pre-condition, $F_{4,16}$=12.8, P<0.001, Sidak's post-test: standard pre-condition vs L741 t_{16}=0.43, P>0.05; standard pre-condition vs cocaine, t_{16}=4.0, P<0.01; cocaine vs cocaine+L741, t_{16}=1.3, P>0.05; cocaine vs lidocaine, t_{16}=3.2, P<0.05). These data suggest that DATs help to support LTCC function in CPu and further emphasise the ability of DAT to regulate DA release through actions on DA axon physiology (Condon et al., 2019) additional to the uptake of DA.

We next explored whether D2Rs limit LTCC control of DA release in NAc. Despite no impact of isradipine on evoked $[DA]_o$ in control conditions (Figure 1G and (Brimblecombe et al., 2015)), in the presence of D2R antagonism, isradipine decreased 1p evoked $[DA]_o$ by ~25% (**Figure 2D,E,** Two-way ANOVA, isradipine x pre-condition interaction, $F_{16,68}$=5.9, P<0.001; effect of pre-condition, $F_{1,68}$=138.4, P<0.0001, Sidak's posttest, standard pre-condition vs L741, P<0.001, comparison of peaks, t-test, t_6=27.6, P<0.001, N=4). The regulation of LTCC control of DA release by D2Rs in NAc was significantly greater than in CPu (**Figure 2F,** Two-way ANOVA, region x D2R, interaction, $F_{1,14}$=8.1, P=0.013; Sidak's post-test, NAc, P<0.01, CPu, P>0.05). The ability of isradipine to decrease DA release in NAc in the presence of D2R antagonism is consistent with studies showing that D2R in other neurons can limit LTCC function. However, our findings are somewhat surprising because D2R antagonists alone do not modify $[DA]_o$ evoked by single stimulation pulses (Condon et al., 2019) suggesting that there is no tonic activity at D2Rs. This disparity suggests that the mechanism by which D2Rs regulate DA release are uncoupled from their regulatory effects of LTCCs.

In NAc, where LTCC function is limited by D2Rs and calb1, we tested whether these regulators intersected or impacted on DAT regulation of LTCCs to further understand the hierarchy of regulatory mechanisms. In NAc of calbKD mice, isradipine decreased $[DA]_o$ to a similar extent (~25%) in control conditions and in the presence of D2R antagonist L-741626 (**Figure 2G-I**). However, in the presence of cocaine, isradipine in CalbKD mice did not decrease $[DA]_o$ (**Figure 2G-I,** Two-way ANOVA, pre-condition x isradipine interaction, $F_{16,68}$=3.34, P=0.0002; comparison of peaks, L741: t-test, t_4=4.3, P=0.012, cocaine: t-test, t_4=1.0, P=0.36). Therefore, in NAc, after calbKD, LTCC function is

not limited by D2Rs. Rather, as seen in CPu, a DAT-dependence of LTCC control is exposed in NAc (**Figure 2I,** One-way ANOVA, $F_{3,9}$=9.5, P=0.004; Sidak's post-test standard conditions vs L741, P>0.05, standard conditions vs cocaine, P<0.05, data from calbWT and calbKD are replicated from Fig 1G). In other words, when LTCCs are contributing to DA release, in either CPu or NAc, their function is supported by the DAT, but under normal conditions in NAc, LTCC function is normally limited by D2Rs and by calb1. It is relevant to note that in NAc of calbKD mice, DA uptake rates are enhanced relative to controls (Brimblecombe et al., 2019), suggesting that LTCC contribution to DA release in NAc might be potentiated in calbKD mice by reduced Ca^{2+} buffering and/or the impact of elevated DAT (e.g. electrogenic effects on depolarisation).

Gabapentinoids limit LTCC function but not DA release

VGCC function depends on the conductance of a diverse range of α_1-pore forming subunits and also on auxiliary subunits including $\alpha_2\delta$, which regulate VGCC levels and position in the presynaptic membrane, and to a lesser extent, voltage-gating properties (Dolphin, 2012). The extensive axonal arbours of DA neurons form ~10^5 DA release sites per neuron, and the trafficking and regulation of VGCCs that supply Ca^{2+} to these sites are likely to be dependent upon $\alpha_2\delta$ subunits, although this has never been explored for DA axons. Here, we tested in DA axons in CPu whether the function of LTCCs, and also other VGCCs more broadly, is regulated by $\alpha_2\delta$ subunits. In particular, we assessed the effects of $\alpha_2\delta$ ligands gabapentinoids (gabapentin, GBP, pregabalin, PGB) that prevent normal interactions between $\alpha_2\delta$ and α_1 subunits.

We first assessed in CPu the effect of GBP on DA release levels. $[DA]_o$ evoked by single pulses and trains were modestly but significantly potentiated by GBP incubation (50 µM) in two different concentrations of extracellular Ca^{2+} ($[Ca^{2+}]_o$) (**Figure 3A,** Two-way ANOVA, effect of GBP: $F_{1,80}$=4.77, *P=0.032,* N=17-25 sites from 4 animals/condition*)* across a range of different stimuli frequencies without affecting the relationship to stimulation frequency (**Figure 3B** Two-way ANOVA effect of GBP $F_{1,20}$=0.017 *P=0.69* N=3 sites from 3 animals). GBP is typically reported to decrease release of other neurotransmitters (Bayer et al., 2004; Maneuf and McKnight, 2001; Quintero et al., 2011), and since DA release is under tonic inhibition by striatal GABA (Lopes et al., 2018), we explored whether GBP might increase DA release by a disinhibition mechanism involving reduced striatal GABA inhibition of DA. However, the effect of combined $GABA_A$ and $GABA_B$ receptor antagonists (bicuculline, 10 µM; CGP 55845, 3.5 µM) to increase evoked $[DA]_o$ did not differ between control vs GBP pre-treated conditions (**Figure 3C**; Two-way ANOVA, effect of GBP, $F_{1,52}$=3.77, *P=0.060*; comparison of peaks in GABA-inhibition with versus without GBP: t-test, t_4=0.63, *P=0.56,* N=3) indicating that an indirect

action on disinhibition is not the means through which GBP promotes DA release, suggesting a direct mechanism.

We next tested whether GBP modified the Ca^{2+}-dependence of DA release. The relationship between $[Ca^{2+}]_o$ and $[DA]_o$ evoked by single pulses was modified by GBP incubation (50 µM): GBP lowered both the EC_{50} (1.97 mM vs 2.19 mM) and Hill slope (1.53 vs 2.05) (**Figure 3D,** comparison of fits, $F_{2,27}$=6.0, *P=0.007,* N=4), indicating that GBP enhances the efficiency of DA release but decreases the cooperativity of Ca^{2+}. A more efficient, yet less cooperative relationship between Ca^{2+} entry and DA release could hypothetically occur if there is a "tighter" coupling of Ca^{2+} entry to DA release, occurring via fewer types of VGCCs. We tested both aspects in turn.

We tested whether GBP tightened the coupling between Ca^{2+} entry and DA release, using the membrane-permeable exogenous Ca^{2+} chelators BAPTA-AM and EGTA-AM, which through fast and slow binding kinetics respectively, have been used in many other synapse types to identify whether sources of Ca^{2+} are tightly or loosely coupled to transmitter release (Eggermann et al., 2012). In control conditions (2.4 mM $[Ca^{2+}]_o$), BAPTA-AM and EGTA-AM reduced evoked $[DA]_o$ in CPu to similar extents (**Figure 3E**) indicating a relatively loose spatiotemporal coupling, as seen previously (Brimblecombe et al., 2015). However, in the presence of GBP or PGB (100 µM), BAPTA-AM decreased evoked $[DA]_o$ to a greater extent than EGTA-AM (**Figure 3F;** Two-way ANOVA, GBP x chelator interaction: $F_{2,46}$=1.1, *P*=0.023; Sidak post-test, GBP: BAPTA-AM vs. EGTA-AM, *P*<0.01, PGB: BAPTA-AM vs EGTA-AM, *P<0.01.* aCSF and GBP: N=12 sites from 4 animals; PGB: N=6 sites from 2 animals). GBP significantly increased the ratio of $[DA]_o$ remaining in EGTA vs BAPTA (from 1.1 ± 0.2 to 2.9 ± 0.5) (not illustrated, unpaired t-test: t_{38}=3.16, *P*=0.003). These data indicate that GBP tightens the spatiotemporal coupling between Ca^{2+} entry and DA release, and thereby provide an explanation for the finding that GBP increases the efficiency of the Ca^{2+} dependence of DA release. It should be noted that although greater effect of BAPTA/EGTA is often attributed to "tighter spatiotemporal coupling" it is also consistent with a broader action potential (Nakamura et al., 2018). Therefore it is possible that GBP is limiting L- and P/Q-type channels from broadening the AP waveform (consistent with Vandael 2012 broader AP waveform in cav1.3-/- in chromaffin cells). Confirmation of the effects of GBP on AP-waveform is non-trivial given the complex and very fine axonal architecture making axonal patching highly complex.

We tested the hypothesis that GBP limits the types of VGCCs that contribute to DA release, including specific testing of whether GBP modulates LTCC function. DA release in striatum normally depends on a broad range of VGCC types including N, P/Q, T and L, with P/Q, T and L types playing a greater (P/Q) or exclusive (T, L) role in CPu compared to NAc (Brimblecombe et al., 2015). We

assessed whether GBP incubation (50 µM) attenuated the effects on DA release of VGCC subtype-specific inhibitors for all four major channel types operating in CPu. In control conditions as seen previously (Brimblecombe et al., 2015), $[DA]_o$ evoked by 1p were significantly decreased by L-channel inhibitor isradipine (5 µM), P/Q-channel inhibitor ω-agatoxin IVA (200 nM), N-channel inhibitor ω-conotoxin GVIA (100 nM), or T-channel inhibitor NNC-055396 (1 µM) (**Figure 3G,H**). Pre-incubation with GBP significantly reduced the effects of isradipine, and ω-ATX IVA, but not other inhibitors: LTCC inhibitor isradipine reduced evoked $[DA]_o$ by 30% in control conditions but not at all in the presence of GBP, and P/Q blocker ω-ATX decreased evoked $[DA]_o$ by 83% in control conditions but by only 32% in the presence of GBP (**Fig 3 G,H;** Two-way ANOVA: effect of GBP, $F_{1,16}$=28.6, P<0.0001; GBP x VGCC interaction: $F_{3,16}$=12.1, P=0.002; Sidak post-test: isradipine, P<0.01; ω-ATX, P<0.001 N=3-4 animals/condition). Similarly, pregabalin (PGB, 100 µM) occluded the effect of isradipine on DA release (**Figure 3I,** comparison of peak max, t-test, t_4=1.1, P=0.33); the effects of PGB on other VGCC blockers were not tested. Gabapentinoids therefore limit the range of VGCCs that support DA release in CPu, and in particular, limit the function of P/Q and L-type channels. Together these data corroborate the hypotheses that gabapentinoids modify DA release in a manner that involves "tighter" coupling of Ca^{2+} entry to DA release occurring via fewer types of VGCCs. They also demonstrate that $\alpha_2\delta$ subunits support LTCC contribution to DA release in CPu. The effect of GBP on P/Q- and L-function but not N-channel function is intriguing. Why GBP does not modify N-channel function in these neurons is not known, but it has been previously found in rat sympathetic neurons that $\alpha_2\delta$ type-1 and -2 subunits promote insertion of P/Q-channels over N-types, whereas $\alpha_2\delta$-3 subunits protect N-type from displacement (Scott and Kammermeier, 2017). Gabapentinoids bind to $\alpha_2\delta$-1 and-2 subunits via their RRR-motif adjacent to the von Willebrand factor A (VWA) domain, but $\alpha_2\delta$-3, in which the RRR-motif is incomplete (Dolphin, 2012), do not bind GBP. We speculate that N-channels in DA axons might associate preferentially with $\alpha_2\delta3$, and therefore remain unaffected by GBP.

GBP has recently been shown to influence NMDA receptor trafficking (Chen et al., 2018), and NMDA receptor activation has been shown to activate LTCCs in immature DA axons (regulating axon growth and branching) (Schmitz et al., 2009). However, the LTCC contribution to DA release from adult DA axons here was independent of NMDA receptors: inclusion of the NMDA receptor antagonist D-APV (50 µM) did not prevent the typical effects of isradipine on evoked $[DA]_o$ (**Figure 3J**; comparison of peak max, t-test, t_4=14.4, P<0.0001) indicating that the effects of GBA shown here on LTCC regulation of DA release are independent of NMDA-receptor mechanisms.

Finally, we tested whether $\alpha_2\delta$ subunits also helped to support the function of LTCCs in NAc in male mice and in CPu in female mice that was exposed by knocking down calb1. Intriguingly, we

found that the effect of isradipine on evoked $[DA]_o$ in NAc that could be detected in male calbKD mice were not prevented by incubation with GBP (**Figure 3K,** comparison of peak max, t-test, t_6=7.6, P=0.0003). By contrast, the effect of isradipine on $[DA]_o$ in CPu of female calbKD mice was attenuated by pre-incubation with GBP (**Figure 3K-L;** comparison of peak max, t-test, t_4=2.5, P=0.07; effect of isradipine significantly different with and without GBP: 2-way ANOVA effect of GBP, $F_{1,10}$=6.0, *P=0.034* with sidak post-test. Data without GBP are from Fig 1E and G). These data indicate that LTCC function is regulated by $\alpha_2\delta$ subunits in DA neurons projecting to dorsal striatum, but not in DA neurons that project to ventral striatum even under conditions that remove other limitations on LTCC function in NAc (calb1). Differences in the VGCC control of DA release between the CPu and NAc cannot therefore be simply explained by calb1.

Our findings that GBP tightens the spatiotemporal coupling between Ca^{2+} sources and DA release, suggest that $\alpha_2\delta$ subunits in DA axons in CPu are normally acting to disperse, or loosen, the overall coupling between VGCC α1-subunits and the DA release machinery. However, given the range of different VGCC types involved, this interpretation is probably over-simplistic. It also differs from previous findings in dissociated rat hippocampal neurons where $\alpha_2\delta$ is thought to tighten the spatial relationship between Ca^{2+} entry and release machinery (Hoppa et al., 2012). Given the selective reduction we saw in function of L- and P/Q function in DA axons, $\alpha_2\delta$ subunits here might be important for recruiting these channels to release sites, shortening their individual distances from the release machinery and tightening their coupling to DA release, but with a net effect of widening the total pool of VGCCs (N, PQ, L and T) that contribute to DA release. GBP, by limiting the recruitment of more peripheral VGCC subtypes (PQ, L) could therefore result in a tighter spatial relationship of the remaining channels to the release machinery (particularly N-type, and a small number of PQ-type channels), and even elevate DA release.

In summary, we have identified that the role of axonal LTCCs in the control of DA release is differentially regulated in dorsal and ventral striatum by several factors, spanning Ca^{2+} binding protein Calb1, D2Rs, the DAT and $\alpha_2\delta$ subunits. These factors vary between striatal regions and account for the disparity between LTCC expression by midbrain DA neurons and LTCC function in neurons and axons. We note also that some of these factors including sex and calb1 have been suggested to confer a change to the risk of PD. We speculate in turn that $\alpha_2\delta$ ligands gabapentinoids, by limiting LTCC function and without compromising DA release, should be explored for a potential neuroprotection of DA neurons, as a new avenue for a neuroprotective strategy against PD.

Materials and methods

Animals

Male and female adult (3-6 months) mice (c57Bl6/J (Charles River). Calbindin-knockdown (CalbKD) animals were generated by crossing homozygous $Calb_{TM2}$ (loxP sites flanking Exon1) (Barski et al., 2002)generously donated by Prof. Meyer (University of Munich) (available from Jax https://www.jax.org/strain/031936 and EMMA: strain name B6.(R1)-Calb1tm2Mpin) with homozygous $DAT^{IRES\mathit{cre}}$, generating double-heterozygous offspring with decreased calb1 expression in DAT-expressing cells. CalbWT control mice were age and sex matched heterozygous $DAT^{IRES\mathit{cre}}$ mice to control for decreased DAT-expression in this line as previously published (Brimblecombe et al., 2019).

Slice preparation

Mice were killed by cervical dislocation, the brains removed, and 300 µm coronal striatal slices prepared as described previously (Brimblecombe et al., 2015), in ice-cold HEPES-based buffer saturated with 95% O_2/5% CO_2, containing in mM: 120 NaCl, 20 $NaHCO_3$, 6.7 HEPES acid, 5 KCl, 3.3 HEPES salt, 2 $CaCl_2$, 2 $MgSO_4$, 1.2 KH_2PO_4, 10 glucose. Slices were incubated at room temperature for ≥ 1 hour in HEPES-based buffer before experiments. All procedures were licensed to be carried out at the University of Oxford under the UK Animals (Scientific Procedures) Act 1986.

Fast-scan cyclic voltammetry (FCV)

Ex vivo DA release was monitored in acute coronal slices using fast-scan cyclic voltammetry (FCV) as previously described (Brimblecombe et al., 2015). Slices were superfused in a recording chamber with bicarbonate-buffered artificial cerebrospinal fluid (aCSF) saturated with 95%O_2/5%CO_2 at 31–33 °C, containing in mM: 124 NaCl, 26 $NaHCO_3$, 3.8 KCl, 0.8-3.6 $CaCl_2$ (as stated), 1.3 $MgSO_4$, 1.3 KH_2PO_4, 10 glucose. Evoked extracellular DA concentration ($[DA]_o$) was monitored by FCV using a Millar voltammeter (Julian Millar, Barts and the London School of Medicine and Dentistry) and single-use carbon-fibre microelectrodes (7-10 µm diameter) fabricated in-house (tip length 50-100 µm). A triangular voltage waveform (range -700 mV to +1300 mV vs. Ag/AgCl) was applied at 800 V/s at a scan frequency of 8 Hz. Electrodes were switched out of circuit between scans. Electrodes were calibrated using 2 µM DA, prepared immediately before calibration using stock solution (2.5 mM in 0.1M $HClO_4$ stored at 4 °C). Signals were attributed to DA due to the potentials of their characteristic oxidation (500-600 mV) and reduction (-200 mV) peaks.

Electrical stimulation

DA recordings were obtained from dorsolateral quadrant of CPu, or nucleus accumbens core (NAc). DA release was evoked by a local bipolar concentric Pt/Ir electrode (25 µm diameter; FHC inc. ME, USA) placed approximately 100 µm from the recording electrode. Stimulus pulses (200 µs duration) were given at 0.6 mA (perimaximal in drug-free control conditions). Stimulations were single pulses (1p) or trains of 5 pulses (5p) at 5-100 Hz as specified and were repeated at 2.5 minute intervals, with 1p stimulations occurring every third stimulation to ensure site stability over time. Each stimulation type was recorded in at least triplicate in each recording site in all experimental conditions. All data were obtained in the presence of the nAChR antagonist, dihydro-β-erythroidine (DHβE, 1 µM) to exclude the powerful modulatory effects of cholinergic interneurons on DA release (Cachope et al., 2012; Rice and Cragg, 2004; Threlfell et al., 2012; Zhou et al., 2001).

GBP incubation

Slices were incubated in either gabapentin-containing aCSF (GBP, 50 µM) or control aCSF for 30 min before being transferred to the recording chamber. The recording electrode was inserted into a non-recording site and an additional 30 min was allowed for the electrode to charge and equilibrate. During this time, the slice was superfused with GBP-containing aCSF (50 µM) or control aCSF. Prior to recording, DHβE (1 µM) was added to the superfusion media. For GBP conditions, GBP (50 µM) was present throughout. The alternative gabapentinoid drug pregabalin (100 µM) was included in the superfusate for 30-45 min prior to recording. The concentration of 50 µM GBP selected was based on previously used concentrations (Dooley et al., 2002; Maneuf and McKnight, 2001; Quintero et al., 2011) and can be approximated to 7 µg/mL CSF levels (based on serum concentrations and partition ratios in mice), which is equivalent to a moderate dose of GBP in people of 900 mg/day (Wamil and McLean, 1994). It should be noted that the relationship between $[DA]_o$ and stimulation frequency in the absence and presence of GBP was conducted at 1.2 mM $[Ca^{2+}]_o$ as the relationship between DA release stimulation frequency is enhanced at lower $[Ca^{2+}]_O$, albeit the relationship remains weak (Brimblecombe et al., 2015; Condon et al., 2019).

Since gabapentinoids act not through acute channel inhibition, but by interfering with VGCC subunit interactions that change channel localization and function, their actions are usually considered to be apparent only after chronic incubation. Relatively acute effects of GBPs are not thought to occur in reduced preparations such as cultured neurons (Cassidy et al., 2014; Hoppa et al., 2012). But the timescale over which GBP acts is likely to vary with experimental conditions. More intact preparations promote $\alpha_2\delta$ function over shorter timescales (Uchitel et al., 2010), and we based our ~1 hour GBP incubation time on previous studies which have identified GBP actions in *ex* vivo slice

preparations from other brain regions (Bayer et al., 2004; Maneuf and McKnight, 2001). The function of $\alpha_2\delta$ subunits is thought to be particularly apparent in situations where there is a high degree of endocytosis/membrane turnover (Tran-Van-Minh and Dolphin, 2010). Notably, a high degree of endocytosis has been shown to occur in dopamine axons in *ex vivo* striatal slices (Gabriel et al., 2013) making it likely that GBP actions will be detected over short time scales in this preparation.

EGTA-AM and BAPTA-AM incubation

Striatal sections were bisected and each hemisphere was incubated for 30 mins at room temperature in aCSF containing 2-hydroypropyl-β-cyclodextrin, 70 µM (Sigma), probenecid, 175 µM, (Sigma), pluronic acid, 0.1% (Life Technologies), and either EGTA-AM, 100 µM (Millipore) or BAPTA-AM, 100 µM (Tocris), or DMSO (vehicle control) (Kukley et al., 2007; Ouanounou et al., 1999) in the absence or presence of GBP (50 µM) . Following pre-incubation, hemispheres were incubated for a further 30 minutes in the recording chamber prior to recording. Recordings were alternated between the EGTA-AM/BAPTA-AM-incubated versus non-incubated slice and at paired recording locations. EGTA-AM/BAPTA-AM effects sizes were obtained from peak $[DA]_o$ expressed as a percentage of control paired site.

Drugs and solutions

BAPTA-AM, dihydro-β-erythroidine (DHβE), GBP, NNC 55-0396, isradipine, ω-Agatoxin IVA and ω-Conotoxin GVIA, were purchased from Ascent Scientific or Tocris UK; pluronic acid from Life Technologies; EGTA-AM from Millipore. All other reagents were purchased from Sigma Aldrich. Stock solutions were made to 1000-2000x final concentrations in H_2O (DHβE, GBP, ω-conotoxin GVIA, ω-Agatoxin IVA and NNC 55-0396, cocaine), DMSO (isradipine, EGTA-AM, BAPTA-AM, L741,626) or ethanol (Lidocaine) and stored at -20°C. Drugs were diluted to their required concentrations in aCSF immediately prior to use. Drug concentrations were chosen in accordance with previous studies(Acevedo-Rodriguez et al., 2014; Brimblecombe et al., 2015)

Data and statistical analysis

Data were acquired and analysed using Axoscope 10.5 (Molecular devices) and Excel macros written locally. Data are expressed as mean ± standard error of the mean (SEM), and *n* = number of animal or number of sites per region (for data in Figure 3). Data from each animal were obtained by averaging at least 3 recordings for each stimulus type and normalising to mean control 1p conditions for each animal. Population means were compared using one- or two-way ANOVA with Sidak post-

test and unpaired t-test where appropriate using GraphPad Prism. Curve fits were done using GraphPad Prism.

Western blot

Mice were culled by cervical dislocation, brains extracted and dissected on ice. The striatum and midbrain was extracted from both hemispheres and snap frozen. Samples were prepared for western blot as previously described (Connor-Robson et al., 2019). Briefly, tissue was homogenised on ice in RIPA buffer containing protease inhibitors (Roche) and protein concentration determined by BCA assay. Following dilution Laemmli buffer was added and samples were boiled for 5 minutes at 95°C. Samples were loaded and ran on 4-15% criterion-TGX gels and transferred to PDVF membranes (BioRad). Membranes were blocked for 1 hour at room temperature and then probed with primary antibody (1:1000 Cell Signalling #13176) overnight at +4°C. After incubation with HRP conjugated secondary antibodies the blot was developed using chemiluminescent HRP substrate.

Acknowledgements

The work was funded by grant support from Parkinson's UK (J-1403; G-1803) and a Clarendon Fund/Christ Church Oxford Studentship to BMR.

Author contributions

KRB and SJC designed research and wrote the paper. KRB, NCR, BMR, CG, RtWN and GK performed experiments and analysed data.

Declarations of interest

The authors declare no competing interests

References

Abel, J.L., and Rissman, E.F. (2012). Location, location, location: Genetic regulation of neural sex differences. Rev. Endocr. Metab. Disord. *13*, 151–161.

Abel, J.M., Witt, D.M., and Rissman, E.F. (2011). Sex differences in the cerebellum and frontal cortex: Roles of estrogen receptor alpha and sex chromosome genes. Neuroendocrinology *93*, 230–240.

Acevedo-Rodriguez, A., Zhang, L., Zhou, F., Gong, S., Gu, H., De Biasi, M., Zhou, F.-M., and Dani, J.A. (2014). Cocaine inhibition of nicotinic acetylcholine receptors influences dopamine release. Front. Synaptic Neurosci. *6*, 19.

Andrade, A., Sandoval, A., González-Ramírez, R., Lipscombe, D., Campbell, K.P., and Felix, R. (2009). The α2δ subunit augments functional expression and modifies the pharmacology of CaV1.3 L-type

channels. Cell Calcium *46*, 282–292.

Barski, J.J., Mörl, K., and Meyer, M. (2002). Conditional inactivation of the calbindin D-28k (Calb1) gene by Cre/loxP-mediated recombination. Genesis *32*, 165–168.

Bayer, K., Ahmadi, S., and Zeilhofer, H.U. (2004). Gabapentin may inhibit synaptic transmission in the mouse spinal cord dorsal horn through a preferential block of P/Q-type Ca2+ channels. Neuropharmacology *46*, 743–749.

Brimblecombe, K.R., Gracie, C.J., Platt, N.J., and Cragg, S.J. (2015). Gating of dopamine transmission by calcium and axonal N, Q, T and L-type voltage-gated calcium channels differs between striatal domains. J. Physiol. *593*, 929–946.

Brimblecombe, K.R., Vietti-Michelina, S., Platt, N.J., Kastli, R., Hnieno, A., Gracie, C.J., and Cragg, S.J. (2019). Calbindin-D28K Limits Dopamine Release in Ventral but Not Dorsal Striatum by Regulating Ca 2+ Availability and Dopamine Transporter Function. ACS Chem. Neurosci. *10*, 3419–3426.

Cachope, R., Mateo, Y., Mathur, B.N., Irving, J., Wang, H.-L., Morales, M., Lovinger, D.M., and Cheer, J.F. (2012). Selective activation of cholinergic interneurons enhances accumbal phasic dopamine release: setting the tone for reward processing. Cell Rep. *2*, 33–41.

Cameron, K.N., Solis, E., Ruchala, I., De Felice, L.J., and Eltit, J.M. (2015). Amphetamine activates calcium channels through dopamine transporter-mediated depolarization. Cell Calcium *58*, 457–466.

Cassidy, J.S., Ferron, L., Kadurin, I., Pratt, W.S., and Dolphin, A.C. (2014). Functional exofacially tagged N-type calcium channels elucidate the interaction with auxiliary α2δ-1 subunits. Proc. Natl. Acad. Sci. U. S. A. *111*, 8979–8984.

Chen, J., Li, L., Chen, S.-R., Zhou, M.-H., Jayaraman, V., and Pan, H.-L. (2018). The α2δ-1-NMDA Receptor Complex Is Critically Involved in Neuropathic Pain Development and Gabapentin Therapeutic Actions. CellReports *22*, 2307–2321.

Chung, A.S., Miller, S.M., Sun, Y., Xu, X., and Zweifel, L.S. (2017). Sexual congruency in the connectome and translatome of VTA dopamine neurons. Sci. Rep. *7*, 11120.

Chung, C.Y., Seo, H., Sonntag, K.C., Brooks, A., Lin, L., and Isacson, O. (2005). Cell type-specific gene expression of midbrain dopaminergic neurons reveals molecules involved in their vulnerability and protection. Hum. Mol. Genet. *14*, 1709–1725.

Condon, M.D., Platt, N.J., Zhang, Y.F., Roberts, B.M., Clements, M.A., Vietti-Michelina, S., Tseu, M.Y.,

Brimblecombe, K.R., Threlfell, S., Mann, E.O., et al. (2019). Plasticity in striatal dopamine release is governed by release-independent depression and the dopamine transporter. Nat. Commun. *10*, 1–15.

Connor-Robson, N., Booth, H., Martin, J.G., Gao, B., Li, K., Doig, N., Vowles, J., Browne, C., Klinger, L., Juhasz, P., et al. (2019). An integrated transcriptomics and proteomics analysis reveals functional endocytic dysregulation caused by mutations in LRRK2. Neurobiol. Dis. *127*, 512–526.

Curl, C.L., Delbridge, L.M.D., and Wendt, I.R. (2008). Sex differences in cardiac muscle responsiveness to Ca2+ and L-type Ca2+ channel modulation. Eur. J. Pharmacol. *586*, 288–292.

Dolphin, A.C. (2012). Calcium channel auxiliary α2δ and β subunits: trafficking and one step beyond. Nat. Rev. Neurosci. *13*, 542–555.

Dooley, D.J., Donovan, C.M., Meder, W.P., and Whetzel, S.Z. (2002). Preferential action of gabapentin and pregabalin at P/Q-type voltage-sensitive calcium channels: Inhibition of K+-evoked [3H]-norepinephrine release from rat neocortical slices. Synapse *45*, 171–190.

Eggermann, E., Bucurenciu, I., Goswami, S.P., and Jonas, P. (2012). Nanodomain coupling between Ca^{2+} channels and sensors of exocytosis at fast mammalian synapses. Nat. Rev. Neurosci. *13*, 7–21.

Gabriel, L.R., Wu, S., Kearney, P., Bellvé, K.D., Standley, C., Fogarty, K.E., and Melikian, H.E. (2013). Dopamine transporter endocytic trafficking in striatal dopaminergic neurons: differential dependence on dynamin and the actin cytoskeleton. J. Neurosci. *33*, 17836–17846.

Gerfen, C.R., Baimbridge, K.G., and Thibault, J. (1987). The neostriatal mosaic: III. Biochemical and developmental dissociation of patch-matrix mesostriatal systems. J. Neurosci. *7*, 3935–3944.

Greene, J.G.J.G., Dingledine, R., Grenamyre, J.T., and Greenamyre, J.T. (2005). Gene expression profiling of rat midbrain dopamine neurons: implications for selective vulnerability in parkinsonism. Neurobiol. Dis. *18*, 19–31.

Guzman, J.N., Sánchez-Padilla, J., Chan, C.S., and Surmeier, D.J. (2009). Robust pacemaking in substantia nigra dopaminergic neurons. J. Neurosci. *29*, 11011–11019.

Guzman, J.N., Sanchez-Padilla, J., Wokosin, D., Kondapalli, J., Ilijic, E., Schumacker, P.T., and Surmeier, D.J. (2010). Oxidant stress evoked by pacemaking in dopaminergic neurons is attenuated by DJ-1. Nature *468*, 696–700.

Guzman, J.N., Ilijic, E., Yang, B., Sanchez-Padilla, J., Wokosin, D., Galtieri, D., Kondapalli, J.,

Schumacker, P.T., and Surmeier, D.J. (2018). Systemic isradipine treatment diminishes calcium-dependent mitochondrial oxidant stress. J. Clin. Invest. *128*, 2266–2280.

Hernández-López, S., Tkatch, T., Perez-Garci, E., Galarraga, E., Bargas, J., Hamm, H., and Surmeier, D.J. (2000). D2 Dopamine Receptors in Striatal Medium Spiny Neurons Reduce L-Type Ca2+ Currents and Excitability via a Novel PLCβ1–IP3–Calcineurin-Signaling Cascade. J. Neurosci. *20*, 8987–8995.

Hoppa, M.B., Lana, B., Margas, W., Dolphin, A.C., and Ryan, T.A. (2012). α2δ expression sets presynaptic calcium channel abundance and release probability. Nature *486*, 122–125.

Ilijic, E., Guzman, J.N., and Surmeier, D.J. (2011). The L-type channel antagonist isradipine is neuroprotective in a mouse model of Parkinson's disease. Neurobiol. Dis. *43*, 364–371.

Ingram, S.L., Prasad, B.M., and Amara, S.G. (2002). Dopamine transporter-mediated conductances increase excitability of midbrain dopamine neurons. Nat. Neurosci.

Kukley, M., Capetillo-Zarate, E., and Dietrich, D. (2007). Vesicular glutamate release from axons in white matter. Nat. Neurosci. *10*, 311–320.

Lee, D., Obukhov, A.G., Shen, Q., Liu, Y., Dhawan, P., Nowycky, M.C., and Christakos, S. (2006). Calbindin-D28k decreases L-type calcium channel activity and modulates intracellular calcium homeostasis in response to K+ depolarization in a rat beta cell line RINr1046-38. Cell Calcium *39*, 475–485.

Lopes, E.F., Roberts, B.M., Siddorn, R.E., Clements, M.A., and Cragg, S.J. (2018). Inhibition of nigrostriatal dopamine release by striatal $GABA_A$ and $GABA_B$ receptors. J. Neurosci. 2028–18.

Maneuf, Y.P., and McKnight, A.T. (2001). Block by gabapentin of the facilitation of glutamate release from rat trigeminal nucleus following activation of protein kinase C or adenylyl cyclase. Br. J. Pharmacol. *134*, 237–240.

Nakamura, Y., Reva, M., and DiGregorio, D.A. (2018). Variations in Ca2+ Influx Can Alter Chelator-Based Estimates of Ca2+ Channel-Synaptic Vesicle Coupling Distance. J. Neurosci. *38*, 3971–3987.

Olson, P.A., Tkatch, T., Hernandez-Lopez, S., Ulrich, S., Ilijic, E., Mugnaini, E., Zhang, H., Bezprozvanny, I., and Surmeier, D.J. (2005). G-protein-coupled receptor modulation of striatal CaV1.3 L-type Ca2+ channels is dependent on a Shank-binding domain. J. Neurosci. *25*, 1050–1062.

Ouanounou, A., Zhang, L., Charlton, M.P., and Carlen, P.L. (1999). Differential modulation of synaptic transmission by calcium chelators in young and aged hippocampal CA1 neurons: evidence for altered

calcium homeostasis in aging. J. Neurosci. *19*, 906–915.

Parkinson Study Group STEADY-PD III Investigators (2020). Isradipine Versus Placebo in Early Parkinson Disease. Ann. Intern. Med. *172*, 591–598.

Poulin, J.-F., Zou, J., Drouin-Ouellet, J., Kim, K.-Y.A., Cicchetti, F., and Awatramani, R.B. (2014). Defining midbrain dopaminergic neuron diversity by single-cell gene expression profiling. Cell Rep. *9*, 930–943.

Prabhavathi, K., Selvi, K.T., Poornima, K.N., and Sarvanan, A. (2014). Role of biological sex in normal cardiac function and in its disease outcome - a review. J. Clin. Diagn. Res. *8*, BE01-4.

Quintero, J.E., Dooley, D.J., Pomerleau, F., Huettl, P., and Gerhardt, G.A. (2011). Amperometric measurement of glutamate release modulation by gabapentin and pregabalin in rat neocortical slices: role of voltage-sensitive Ca2+ α2δ-1 subunit. J. Pharmacol. Exp. Ther. *338*, 240–245.

Rice, M.E., and Cragg, S.J. (2004). Nicotine amplifies reward-related dopamine signals in striatum. Nat. Neurosci. *7*, 583–584.

Schmitz, Y., Luccarelli, J., Kim, M., Wang, M., and Sulzer, D. (2009). Glutamate controls growth rate and branching of dopaminergic axons. J. Neurosci. *29*, 11973–11981.

Scott, M.B., and Kammermeier, P.J. (2017). CaV2 channel subtype expression in rat sympathetic neurons is selectively regulated by α2δ subunits. Channels *11*, 555–573.

Sonders, M.S., Zhu, S.J., Zahniser, N.R., Kavanaugh, M.P., and Amara, S.G. (1997). Multiple ionic conductances of the human dopamine transporter: The actions of dopamine and psychostimulants. J. Neurosci.

Surmeier, D.J., Guzman, J.N., and Sanchez-Padilla, J. (2010). Calcium, cellular aging, and selective neuronal vulnerability in Parkinson's disease. Cell Calcium *47*, 175–182.

Threlfell, S., Lalic, T., Platt, N.J., Jennings, K.A., Deisseroth, K., and Cragg, S.J. (2012). Striatal dopamine release is triggered by synchronized activity in cholinergic interneurons. Neuron *75*, 58–64.

Tran-Van-Minh, A., and Dolphin, A.C. (2010). The alpha2delta ligand gabapentin inhibits the Rab11-dependent recycling of the calcium channel subunit alpha2delta-2. J. Neurosci. *30*, 12856–12867.

Uchitel, O.D., Di Guilmi, M.N., Urbano, F.J., and Gonzalez-Inchauspe, C. (2010). Acute modulation of calcium currents and synaptic transmission by gabapentinoids. Channels (Austin). *4*, 490–496.

Vega-Vela, N.E., Osorio, D., Avila-Rodriguez, M., Gonzalez, J., García-Segura, L.M., Echeverria, V., and Barreto, G.E. (2017). L-Type Calcium Channels Modulation by Estradiol. Mol. Neurobiol. *54*, 4996–5007.

Wamil, A.W., and McLean, M.J. (1994). Limitation by gabapentin of high frequency action potential firing by mouse central neurons in cell culture. Epilepsy Res. *17*, 1–11.

Wooten, G.F., Currie, L.J., Bovbjerg, V.E., Lee, J.K., and Patrie, J. (2004). Are men at greater risk for Parkinson's disease than women? J. Neurol. Neurosurg. Psychiatry *75*, 637–639.

Zhou, F.M., Liang, Y., and Dani, J.A. (2001). Endogenous nicotinic cholinergic activity regulates dopamine release in the striatum. Nat. Neurosci. *4*, 1224–1229.

Figure legends

Figure 1. LTCC control of DA release is regulated by calb1 in a regional and sexually dimorphic manner.

(**A**) Mean $[DA]_o$ ± SEM vs time evoked by single pulses (*arrow*) in CPu in control and isradipine (5 µM) (*red*) conditions in male (*left*) and female (*right*), normalised to control. (**B**) Peak $[DA]_o$ ± SEM normalised to pre-isradipine control vs time. (**C**) Representative examples of Western blots for 3 male and 3 female showing actin (42 kDa) and Calb1 (25 kDa). (**D**) Calbindin-D28K/β-actin protein ratios in male and female midbrain and striatum. Mean ± SEM; same colours indicate technical replicates blue points from blot shown in C and are samples on which stats correspond to, N=3. (**E,F,G**) Mean $[DA]_o$ ± SEM vs time evoked in (E) female CPu or (F) male CPu or (G) male NAc, by single pulses (*arrow*) in control (*black*) and isradipine (5 µM) (*red*) in calbWT (*left*) and calbKD (*center*), normalised to control. *Right*, peak $[DA]_o$ in isradipine. *P<0.05, *** P<0.001

Figure 2. LTCC control of DA release can be silenced by D2R in NAc and supported by DATs.

(**A,D,G**) Peak $[DA]_o$ ± SEM normalised to pre-isradipine condition vs time evoked by single pulses in (A) CPu, (D) NAc, and (G) NAc in calbKD before during isradipine application, in a the presence of a standard control pre-condition (*black*), or L741-626, 1 µM (*blue*), or cocaine, 5 µM (*green*). (**B,E,H**) Mean $[DA]_o$ ± SEM vs time evoked by single pulses (*arrow*)

before and after isradipine in CPu (B), NAc (E) and calbKD NAc (H). Additional drugs present as indicated. (**C,F,I**) Peak $[DA]_o$ in isradipine. *P<0.05, **P<0.01.

Figure 3. Targeting $\alpha_2\delta$ subunits of VGCCs with gabapentinoids changes the relationship between $[Ca^{2+}]_o$, VGCCs and DA release

(**A**) Peak $[DA]_o$ evoked by 1p with and without GBP. Bars show mean ± SEM. (**B**) *Left,* Mean $[DA]_o$ ± SEM vs time evoked by 1p and 5p/100Hz at 1.2 mM $[Ca^{2+}]_o$; insert, typical voltammograms. *Right,* Mean ratio ± SEM of peak $[DA]_o$ evoked by 5p at 5-100 Hz versus 1p. (**C**) Peak $[DA]_o$ vs time with application of $GABA_{A/B}$ receptor antagonists (bicuculline, 10 µM, CGP 55845, 4 µM) in the absence and presence of GBP. (**D**) Peak $[DA]_o$ evoked by 1p vs $[Ca^{2+}]_o$, normalised to the 2.4 mM Ca^{2+} condition, with and without GBP. Comparison of fits, ***P<0.001. (**E**) Mean profiles of $[DA]_o$ ± SEM vs time evoked by 1p, in the absence (upper) or presence (lower) of GBP, in the absence (control) and presence of either BAPTA-AM, 100 µM (*left, blue*) or EGTA-AM, 100 µM (*right, green*). Data are normalised to pre-chelator control conditions. (**F**) Peak $[DA]_o$ (% of pre-chelator control) remaining after incubation with BAPTA-AM or EGTA-AM, in the absence or presence of control versus GBP. N=4 animals. Two-way ANOVA, Sidak post-tests. (**G**) Mean profiles of $[DA]_o$ ± SEM evoked by 1p (*arrow*) in the absence (*upper*) or presence of GBP (*lower*), with and without VGCC blockers. Normalised to control conditions prior to VGCC block. L-block, isradipine 5 µM (*red*); P/Q-block, ω-ATX IVA 200nM (*green*); N-block, ω-CTX GVIA 100 nM (*blue*); T-type block, NNC55-0396 1 µM (*yellow*). T-tests, control vs drug. (**H**) Peak $[DA]_o$ after VGCC block. Two-way ANOVA with sidak Post-test. (**I,J**) Mean profiles of $[DA]_o$ ± SEM evoked by 1p in CPu in the presence of (I) PGB (100 µM, black), or (J) NMDA receptor antagonist D-AP-5, plus isradipine 5 µM (*red*). (**K**) Mean profiles of $[DA]_o$ ± SEM evoked by 1p in the presence of GBP (black), plus isradipine in (left) NAc of male CalbKD male mice, or (right) CPu of calbKD female mice. (**L**) Peak $[DA]_o$ in the presence of isradipine in the absence and presence of GBP. Two-way ANOVA with Sidak's posttest. **P*<0.05, ***P*<0.01, ****P*<0.0001.

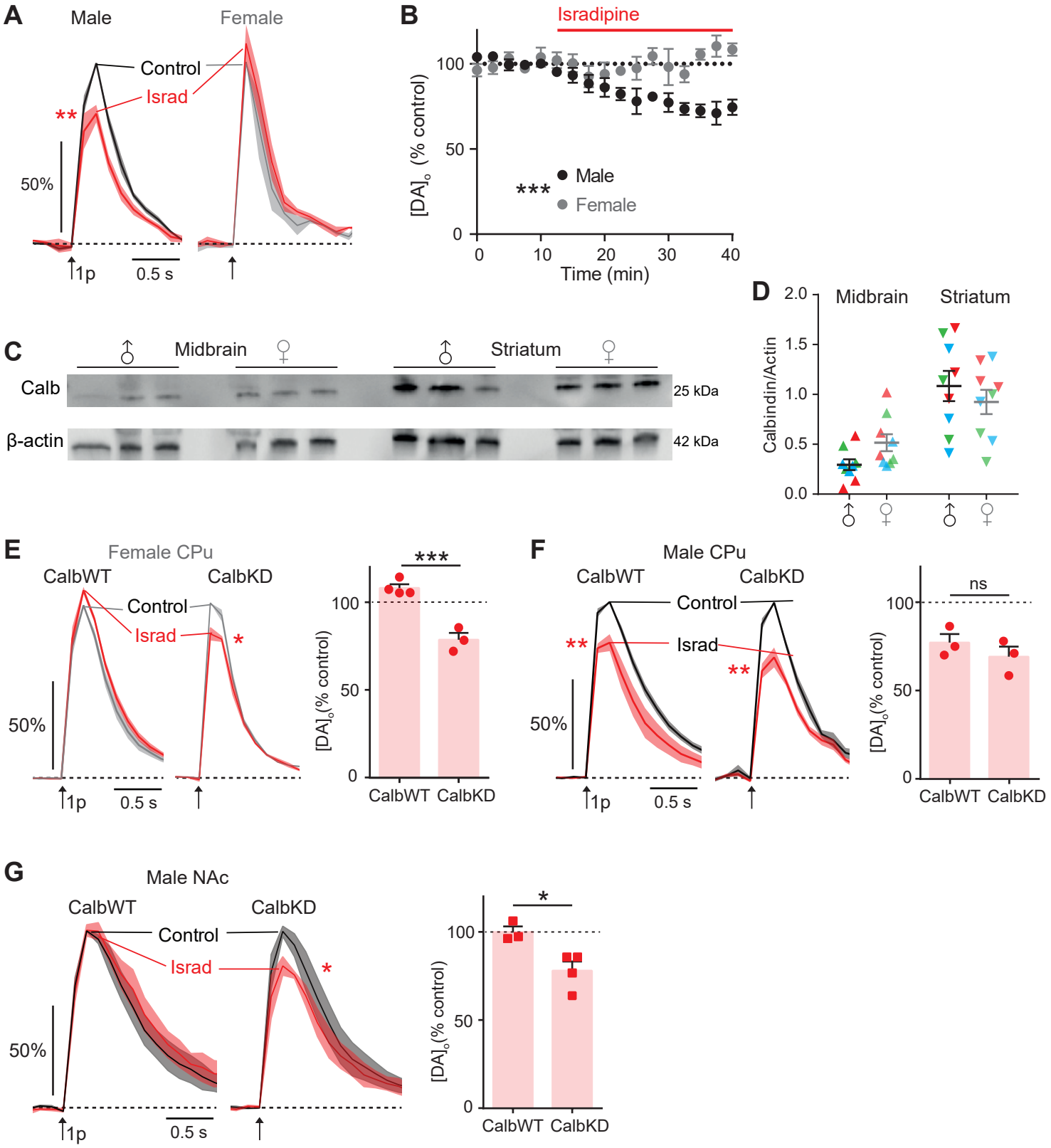

Figure 1 Brimblecombe et al

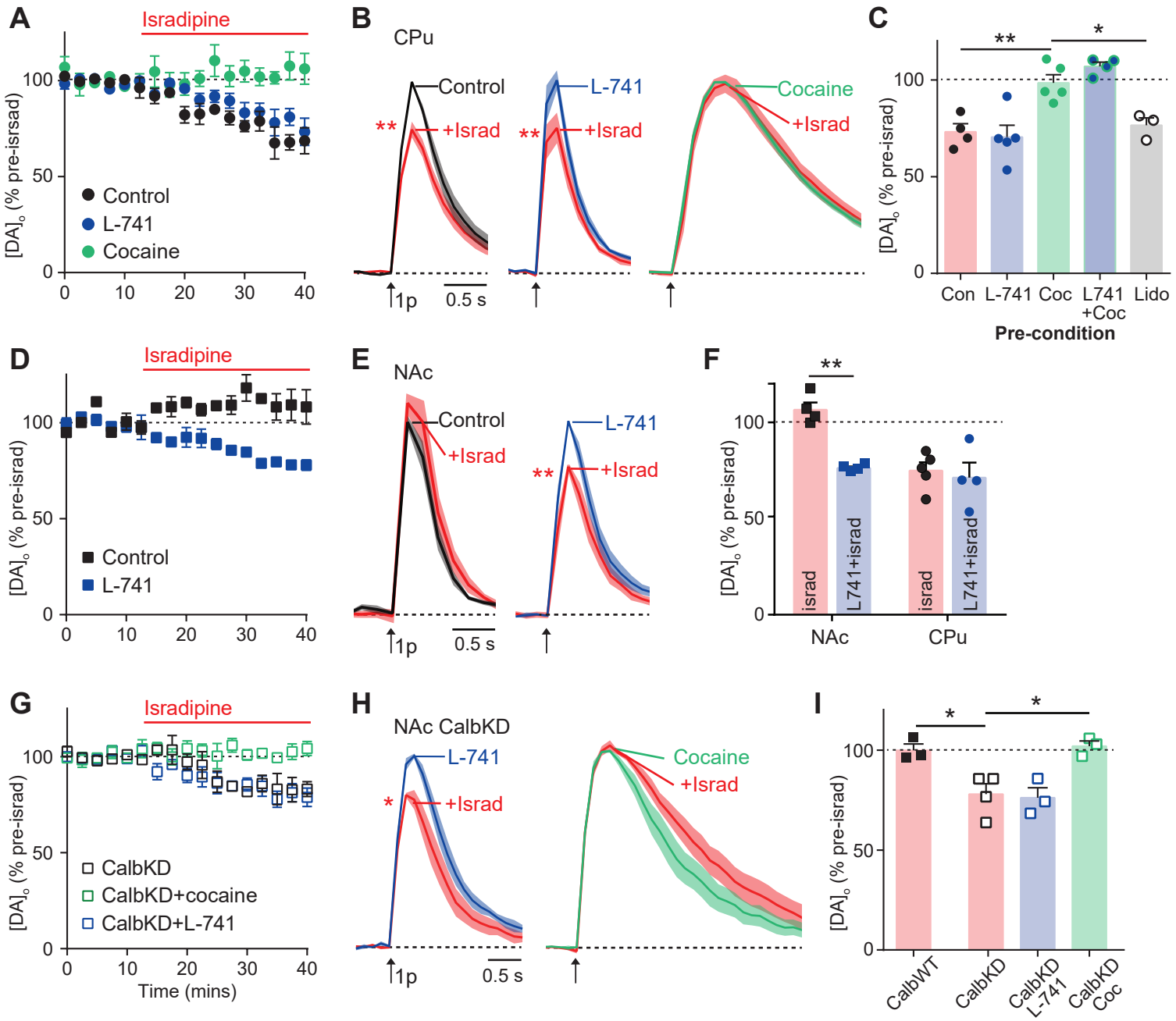

Figure 2 Brimblecombe et al

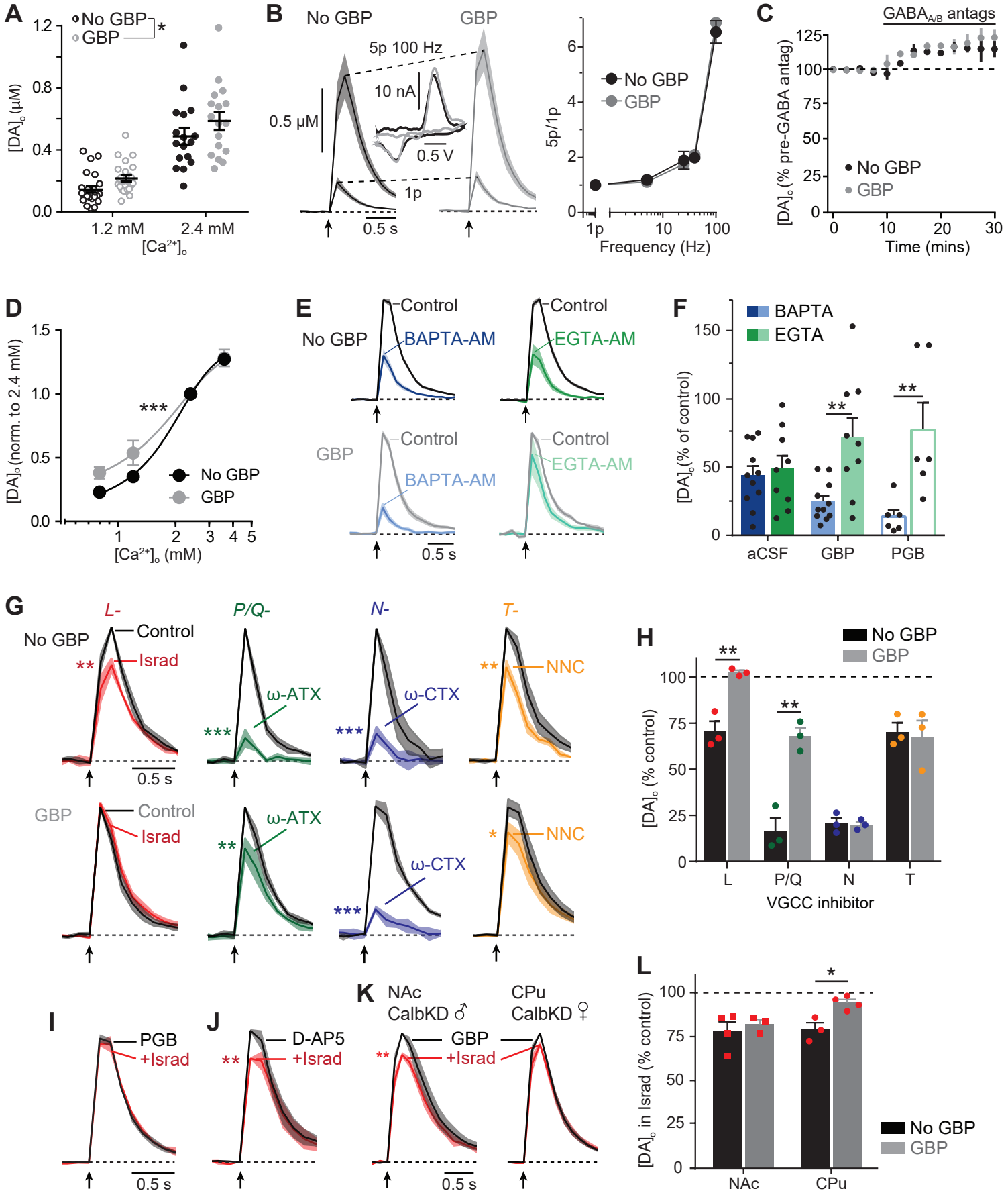

Figure 3 Brimblecombe et al